Carbon nitride frameworks and dense crystalline polymorphs

Chris J. Pickard,[1,2,*] Ashkan Salamat,[3,4] Michael J. Bojdys,[5,6,7] Richard J. Needs,[8] and Paul F. McMillan[9]
[1]*Department of Physics & Astronomy, University College London, Gower Street, London WC1E 6BT, UK*
[2]*Department of Materials Science & Metallurgy, University of Cambridge, 27 Charles Babbage Road, Cambridge CB3 0FS, UK*
[3]*Lyman Laboratory of Physics, Harvard University, Cambridge, Massachusetts 02138, USA*
[4]*Department of Physics and Astronomy and HiPSEC, University of Nevada Las Vegas, Las Vegas, Nevada 89154, USA*
[5]*Charles University in Prague Faculty of Science, Hlavova 8, 128 43 Praha 2, Czech Republic*
[6]*Institute of Organic Chemistry and Biochemistry ASCR, v.v.i. Flemingovo nám. 2, CZ-166 10 Prague 6, Czech Republic*
[7]*Head of the Functional Nanomaterials Group Joint laboratory of IOCB and Charles University in Prague, Czech Republic*
[8]*Theory of Condensed Matter Group, Cavendish Laboratory, J. J. Thomson Avenue, Cambridge CB3 0HE, UK*
[9]*Department of Chemistry, Christopher Ingold Laboratory, University College London, Gordon Street, London WC1H 0AJ, UK*
(Received 10 February 2016; revised manuscript received 18 June 2016; published 8 September 2016)

We used *ab initio* random structure searching (AIRSS) to investigate polymorphism in C_3N_4 carbon nitride as a function of pressure. Our calculations reveal new framework structures, including a particularly stable chiral polymorph of space group $P4_32_12$ containing mixed sp^2 and sp^3 bonding, that we have produced experimentally and recovered to ambient conditions. As pressure is increased a sequence of structures with fully sp^3-bonded C atoms and three-fold-coordinated N atoms is predicted, culminating in a dense $Pnma$ phase above 250 GPa. Beyond 650 GPa we find that C_3N_4 becomes unstable to decomposition into diamond and pyrite-structured CN_2.

DOI: 10.1103/PhysRevB.94.094104

I. INTRODUCTION

Carbon nitrides with N:C ratios >1 form a class of solid-state compounds with properties that are being investigated for applications ranging from gas sorption and catalysis to energy conversion and storage [1–6]. Experimentally known structures are based on sp^2-bonded carbon atoms and include polymeric to graphitic layered compounds. Within the C-N-H system, materials related to Liebig's melon [$(C_6N_9H_3)_n$] contain tri-*s*-triazine (heptazine: C_6N_7) structural units linked via–NH–groups [1,2,7–9]. Additional graphitic materials containing intercalated Li^+, Cl^-, and Br^- ions are formed by polytriazine imide (PTI) layers consisting of triazine (C_3N_3) rings linked by –N= or –NH– species [10–13]. Synthesis of macroscopic flakes of triazine-based graphitic carbon nitride (TGCN) composed of nitrogen-linked triazine (C_3N_3) units was reported recently [14]. This structure was first proposed in the mid-1990s as "graphitic carbon nitride" ("g-C_3N_4") by analogy with the structurally related graphite [15,16]. A nanocrystalline material with C_3N_4 stoichiometry had been reported from chemical vapor deposition [17,18] and related models were studied theoretically [16,19,20]. Triazine-based carbon nitrides can also be exfoliated to produce layered materials analogous to few-layered graphene [21,22]. Theory shows that the optical band gap (1.6–2.7 eV), important in photocatalysis, can be tuned by controlling the layer buckling at high pressure [23,24].

Interest in dense carbon nitride polymorphs based on sp^3 bonded C atoms began with predictions from density functional theory (DFT) calculations of superhard properties [16,25–28]. First investigations began by considering known structures such as those of Si_3N_4 ceramic phases, and more recently by using structure searching methods [29]. However none of the predicted high-density C_3N_4 polymorphs have been demonstrated experimentally to date [1,30]. One carbon nitride solid containing sp^3 bonded C atoms was produced by laser heating dicyandiamide (DCDA: $C_2N_4H_4$) at $P > 27$ GPa in a diamond anvil cell [31]. This material with a defective wurtzite structure could be recovered to ambient conditions [32]. A recent study has identified formation of a CN phase that also contains sp^3 bonded carbon [33].

Experimental compression studies and DFT calculations have also revealed the existence of carbon nitride structures containing both sp^2 and sp^3 bonded C atoms obtained from the graphitic layered PTI compound $C_6N_9H_3 \cdot HCl$. Layer buckling causes C–N distances in adjacent layers to approach a covalently bonded value and an interlayer bonded (ILB) form becomes stabilized above 47 GPa [34]. This result shows that carbon-nitride-framework structures containing mixed sp^2 and sp^3 bonding can exist over a range of densities. Microporous carbon nitride solids have also been produced at ambient pressure by linking C_3N_3 triazine units into three-dimensional covalent networks [35–39].

The structural polymorphism of sp^3-bonded carbon nitride is usefully compared with that of elemental carbon. Here high-pressure synthesis is well known to produce dense structures [40]. Low-pressure allotropes dominated by sp^2 bonding consist of planar graphite and graphene structures formed from fused six-membered rings. Introducing curvature into the layers leads to fullerenes and C nanotubes, while hierarchical low-density mesoporous solids assembled at different length scales are important for nanotechnology and planetary science [40–42]. Theoretical modeling now also points to the potential existence of metastable zeolitic sp^3-bonded carbon-framework structures in the 0–20 GPa range [43]. In equilibrium at low temperatures and pressures above 0.76 GPa [44,45] the dense sp^3-bonded structure of diamond becomes the most stable form and no further structural transformations are expected until a body-centered (BC8) polymorph is predicted above 1000 GPa (1 TPa) [40]. Other new dense allotropes relevant to understanding C-rich

*cjp20@cam.ac.uk

TABLE I. (Top) Comparison of cell parameters for the $P4_32_12$ structure of C_3N_4 at $P = 0$ as determined by experiment and theory (LDA, PBEsol, and PBE). (Bottom) Fractional atomic coordinates from the PBEsol functional. The data in this table were calculated with a very fine k-point spacing of $2\pi \times 0.03$ Å^{-1}.

Cell parameters	Experiment	Theory (LDA)	Theory (PBEsol)	Theory (PBE)
a (Å)	4.021	4.0811	4.1106	4.1375
b (Å)	4.021	4.0811	4.1106	4.1375
c (Å)	13.922	14.0490	14.1978	14.3579
c/a	3.46	3.442	3.454	3.470
V/f.u. (Å^3)	56.29	58.50	59.975	61.45
Fractional coordinates		x	y	z
C1		0.38982	0.20842	0.66623
N2		0.24805	0.13808	0.74384
N3		0.22802	0.29442	0.58513
C4		0.90820	0.09180	0.75000

exoplanets are predicted to exist at extreme pressures extending into the TPa range [46–48].

Here we used *ab initio* random structure searching (AIRSS) [49,50] to explore carbon nitride polymorphism as a function of density throughout a wide pressure range extending between 0–1000 GPa (0–1 TPa), focusing on behavior at the C_3N_4 composition. At low density the results reveal new crystalline architectures including previously unsuspected framework structures based on mixed sp^2-sp^3 bonding. One of these structures ($P4_32_12$ or its enantiomorph $P4_12_12$) has been verified experimentally in our study. The AIRSS results allow a ranking of stability among predicted C_3N_4 polymorphs up to 650 GPa, above which C_3N_4 becomes unstable relative to diamond + pyrite-structured CN_2.

II. STRUCTURE SEARCHING

AIRSS is a powerful theoretical prediction technique that has led to the discovery of new structures subsequently verified by experiment, in materials ranging from hydrogen [51,52], ammonia [53], ammonia hydrates [54,55], aluminium hydride [56], and silane [49] to xenon oxides [57]. Within the AIRSS method, a cell volume and shape are selected at random, atoms are added at random positions to provide the desired composition, and the system is relaxed until the forces on the atoms are negligible and the pressure takes the required value. This procedure is repeated many times, giving a relatively sparse sampling of the "structure space." We typically constrain the minimum separations between atom pairs (C–C, C–N, N–N) in the initial structures, which helps to space out the atoms appropriately, while retaining a high degree of randomness. These minimum distances are obtained from preliminary short AIRSS runs. In almost all of the subsequent searches we impose symmetry constraints on the structures; for example, we might demand that all structures belong to randomly selected space groups with eight or more symmetries. In the next stage of searching we might choose to allow structures with four or more symmetries, etc. With this approach we obtain a very good sampling of the high-symmetry structures, which can be extended towards lower symmetries as the available computing resources allow. The use of symmetry constraints greatly reduces the size of the "structure space," although they also break it up into disconnected regions which can prevent some structures from relaxing fully. However, there is a strong tendency for low-energy structures to possess symmetry [58], and we find that the application of symmetry constraints throughout the searching is a very useful tool. Searches for low-pressure structures are performed using heptazine- and triazine-based units and we consider structures containing up to sixteen formula units (f.u.).

The structure searches were performed by using AIRSS and first-principles DFT methods, version 8.0 of the CASTEP plane-wave basis-set pseudopotential code [59], default CASTEP ultrasoft pseudopotentials [60], a plane-wave basis-set energy cutoff of 280 eV, and an initial Brillouin-zone sampling grid of spacing $2\pi \times 0.1$ Å^{-1}. The PBE generalized gradient approximation density functional [61] was used for the structure searches. The final numerical results reported in this paper were obtained by using the PBEsol functional with a basis-set energy cutoff of 700 eV, CASTEP "on-the-fly" ultrasoft pseudopotentials, as described in the supplemental material [62], and a k-point spacing of $2\pi \times 0.05$ Å^{-1}, except for the data in Table I, which were calculated with a finer k-point spacing of $2\pi \times 0.03$ Å^{-1}.

III. CHOICE OF DENSITY FUNCTIONAL

Estimating the pressure of polymorphic transitions among sp^2- and sp^3-bonded phases for carbon nitride materials is difficult because no reliable data for the structures and energetics of sp^3-bonded C_3N_4 polymorphs are available. To choose a density functional that would provide reasonable transition pressures for comparison with experiment we considered the well-known transition from sp^2-bonded graphite to sp^3-bonded diamond in elemental carbon, which has distinct similarities to C_3N_4. The structures and lattice constants of diamond and graphite are known, which allows accurate comparisons to be made with the results of DFT calculations [44,45].

In Fig. 1 we plot the differences in enthalpy between the graphite and reference diamond structures calculated using five density functionals: the local density approximation (LDA) [63], the semilocal PBE [61], WC [64] and PBEsol

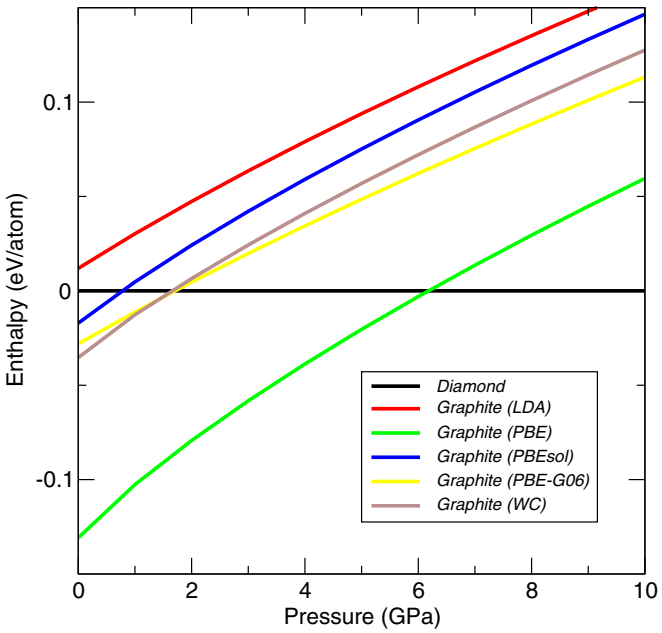

FIG. 1. Enthalpy per atom for carbon graphite relative to diamond as a function of pressure calculated by using five different density functionals (LDA, PBE, PBEsol, PBE + G06, and WC).

generalized gradient approximations [65], and the PBE + G06 generalized gradient approximation with empirical van der Waals corrections [61,66]. The calculated graphite-diamond transition pressures ranged from -1 GPa (LDA) to +6 GPa (PBE), which provides an estimate of the range of errors in the pressure arising from the approximate density functionals of about ±4 GPa, see Fig. 1.

The most important factor for obtaining an accurate graphite-diamond transition pressure is to use a functional that provides a good account of the volume of diamond and the in-plane lattice constant of graphite. Here, the effects of zero-point vibrational motion are estimated to be small and have been neglected. The LDA normally tends to underestimate volumes, while PBE tends to overestimate them. PBEsol, WC, and PBE + G06 give volumes for diamond intermediate between those of LDA and PBE and are in reasonable agreement with experiment. The description of graphite is more variable. The graphite-diamond transition pressure is calculated to be 0.7 GPa by using PBEsol, in close agreement with experiment. WC and PBE-G06 both give 2 GPa, while PBE predicts the transition at 6 GPa. We therefore elected to use PBEsol for our studies of C_3N_4 polymorphs. The PBE and PBEsol functionals gave the same sequence of polymorphic phase transitions, although the PBEsol transition pressures are somewhat larger.

IV. STRUCTURES FOUND IN THE HIGH-PRESSURE SEARCHES

Enthalpy-pressure relations for C_3N_4 polymorphs found by AIRSS using the PBEsol functional are shown in Fig. 2. Below approximately 5 GPa we find that carbon nitride compounds are metastable with respect to elemental carbon (diamond or graphitic polymorphs) and N_2 phases. At low pressure a wide variety of corrugated layers or open framework structures based on linked heptazine or triazine motifs are predicted to occur and the number of potential polymorphs and structure types increases dramatically with system size [67]. These low-density materials typically have very large unit-cell volumes and they rapidly become destabilized with increasing pressure [29]. The importance of such mesoporous phases and their relationship to layered and framework-structured carbon nitrides is discussed below. Heptazine-based structures of Cc, $Fdd2$, and $Pbca$ symmetries are the most stable below 2 GPa in PBEsol, and the $P4_32_12$ structure with mixed sp^2-sp^3 bonding is stable in the range 2–11 GPa. At higher pressures, we find structures with sp^3 bonding around the carbon atoms to be the most stable. We found the following sequence of transitions among the most stable phases as a function of pressure:

$$Cc \xrightarrow{0.05} Pbca \xrightarrow{2} P4_32_12 \xrightarrow{11} P31c \xrightarrow{47} Pnnm \xrightarrow{100}$$
$$Pmc2_1 \xrightarrow{106} I\bar{4}2m \xrightarrow{172} I\bar{4}3d \xrightarrow{195} Cmc2_1 \xrightarrow{238} Pnma.$$

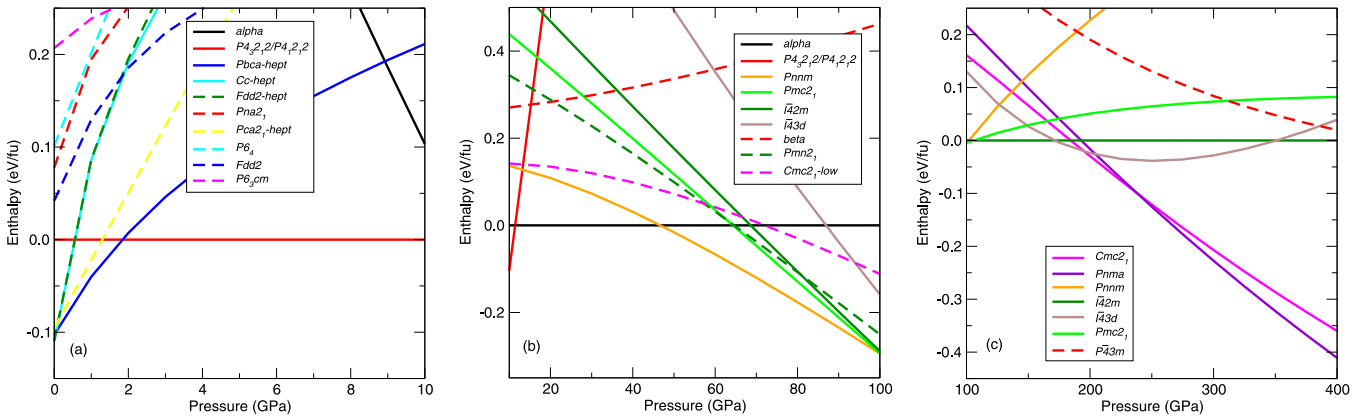

FIG. 2. PBE Enthalpy versus pressure in C_3N_4 in pressures up to 400 GPa. Enthalpy per atom using the PBEsol functional as a function of pressure for C_3N_4 polymorphs identified by AIRSS. The solid lines indicate phases that are predicted to have stable regions in the range shown. Results are shown in three pressure ranges to highlight polymorphism at low (0–10 GPa), intermediate (10–100 GPa), and high (100–400 GPa) pressures. In panel (a) the enthalpies are plotted relative to the $P4_32_12$ framework polymorph, whereas in panel (b) the α-C_3N_4 structure is used as a reference state. In panel (c) the $I\bar{4}2m$ structure is taken as the reference.

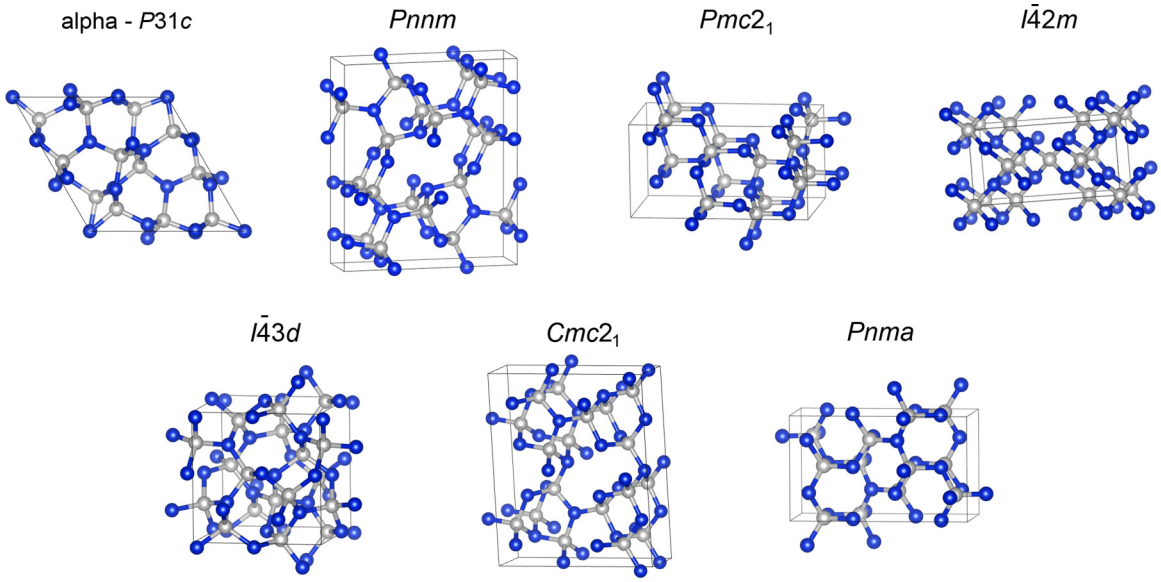

FIG. 3. Structures formed at intermediate and high pressure in the C_3N_4 system. N atoms are depicted as blue spheres and C atoms are gray. The α-C_3N_4 ($P31c$) phase is predicted by PBEsol to be stable between 11–47 GPa, followed by $Pnnm$, $Pmc2_1$, $I\bar{4}2m$, $I\bar{4}3d$, $Cmc2_1$, and $Pnma$ polymorphs at the transition pressures given in the text.

The numbers above the arrows indicate the PBEsol transition pressures in GPa. (The Cm structure found in DFT searches by Dong *et al.* [29] is not predicted to be stable at any pressure because our study has discovered new structures that are more stable.)

Structures of the high-density phases predicted to become stable at high pressure are illustrated in Fig. 3. The low-enthalpy structures contain only C–N bonds, no C–C or N–N bonding was found to occur in energetically competitive structures over the pressure range studied of 0–1 TPa. Between 11–47 GPa (using PBEsol), the α-C_3N_4 structure with $P31c$ symmetry analogous to the ceramic phase α-Si_3N_4 is predicted to be stable. This is one of the polymorphs considered by Cohen, Sung, and others to constitute a likely ultralow compressibility, superhard material [16,25–28]. The α-C_3N_4 structure contains sp^3 bonded four-coordinated C atoms and sp^2 bonded three-fold-coordinated N atoms characteristic of other low-enthalpy structures at high pressures. In addition to its low compressibility and potentially high hardness it has been predicted to have the interesting materials property of a negative Poisson's ratio [68]. The β-C_3N_4 phase considered in early discussions is not stable at any pressure within the range studied. Above 47 GPa we find that α-C_3N_4 is overtaken in stability by a $Pnnm$ structured phase that remains the most stable polymorph until 100 GPa (Fig. 3). At this pressure a structure with $Pmc2_1$ symmetry makes a brief appearance, before the introduction of a cubic ($I\bar{4}2m$) structure [29] containing nearly tetrahedrally bonded N atoms along with the sp^3-bonded C-atom centers. Neither the $Pnnm$ nor $Pmc2_1$ polymorphs were identified as stable phases in structure searches reported by Dong *et al.* [29]. At 195 GPa another cubic ($I\bar{4}3d$) phase makes a brief appearance, followed by a $Cmc2_1$ structured polymorph that is stable until 238 GPa. This phase was described by Dong *et al.* as occurring between 224 and 300 GPa. It appears to resolve the competing structural situation between C- and N-based bonding with the emergence of clearly separated C- and N-atomic layers within a structure that could be described as "defective" diamond or c-BN. Above 238 GPa the most stable predicted polymorph has orthorhombic $Pnma$ symmetry. This remains the most stable phase until 650 GPa where it decomposes into diamond and a pyrite-structured CN_2 polymorph according to

$$C_3N_4(Pnma) \rightarrow \text{C(diamond)} + 2CN_2(Pa\bar{3},\text{pyrite}).$$

V. DIAMOND ANVIL CELL EXPERIMENTS

To begin to test our theoretical predictions we carried out an exploratory synthesis experiment in a laser-heated diamond anvil cell (DAC), using a sample of crystalline TGCN g-C_3N_4 as a starting material [14]. This compound has been shown to have $P6_3cm$ or $P\bar{6}m2$ symmetry corresponding to ABC or AB stacking of the buckled graphitic layers. A thin sample flake of approximately 60 × 60 micrometers in lateral dimensions was loaded into the DAC chamber and isolated from the diamond window by using three small ruby spheres. The pressure was determined by ruby fluorescence from a different ruby sphere placed away from the sample. The sample was compressed by using Ne as the pressure-transmitting medium (PTM). *In situ* x-ray diffraction experiments were carried out at beamline ID27 of the European Synchrotron Radiation Facility by using monochromatic radiation (λ = 0.3738 Å). The starting material exhibits an intense peak at $2\theta = 6.6^\circ$ due to the 002 reflection of the g-C_3N_4 TGCN phase [Fig. 4(a)]. During initial compression to 53 GPa this peak first shifts to larger 2θ values then broadens and finally disappears above approximately 40 GPa [Fig. 4(a)]. This most likely occurs due to structural disordering associated with layer buckling and possible interlayer C-N bonding at high pressure as previously observed for structurally related $C_6N_9H_3 \cdot HCl$ [34]. By 53 GPa the only peaks remaining in the pattern correspond to the face-centered-cubic lattice of solid Ne used as the PTM [Fig. 4(a)].

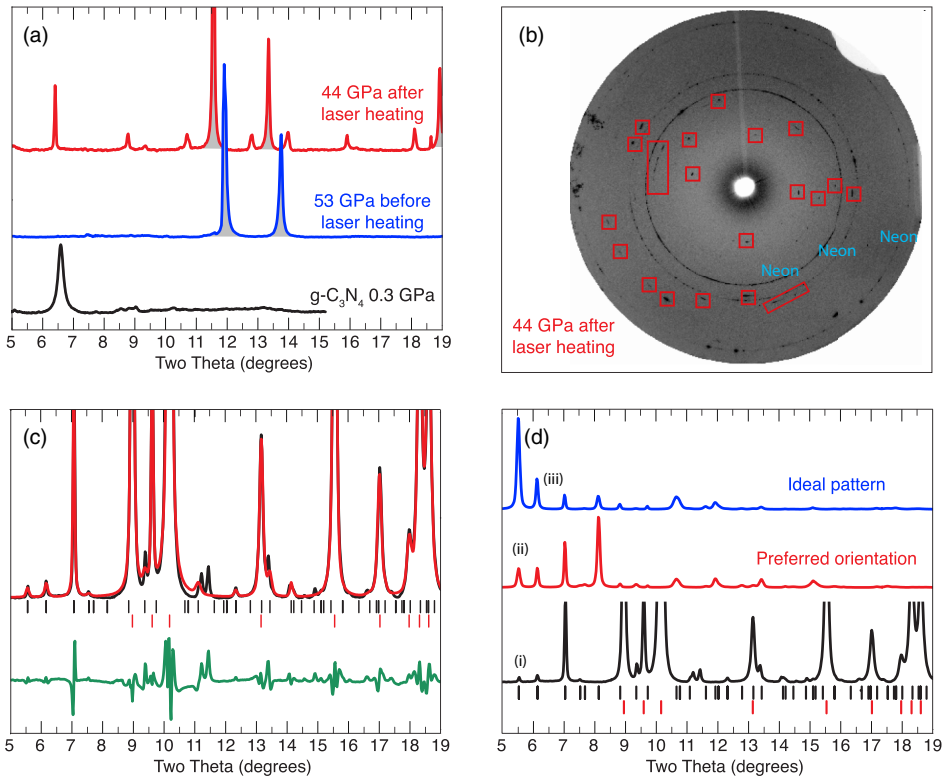

FIG. 4. Experimental x-ray diffraction data. (a) Starting C_3N_4 sample before and after laser heating at various pressures. Peaks with shaded gray areas are from the Ne pressure transmitting medium. (b) Diffraction image at 44 GPa after laser heating at 1500 K. The emergence of new crystalline features are highlighted in red boxes. The three Debye–Scherrer diffraction rings due to the Ne pressure-transmitting medium are labelled. (c) Le Bail refinement of the recovered $P4_32_12$ (or $P4_12_12$) phase of C_3N_4. Data points and Le Bail fits are overlaid in black and red, respectively, and a difference plot is shown. The experimental pattern contains a contribution from the Re gasket material that remained present surrounding the sample. Top (black) and bottom (red) tick marks are for the C_3N_4 phase and Re, respectively. (d) (i) The plot shows the experimental data obtained at ambient conditions. (ii) The plot depicts a simulated pseudo-Rietveld refinement of the data assuming a composite of oriented crystallites with fixed atomic positions taken from the theoretical study (Table I). (iii) The plot shows the calculated powder pattern expected from complete sampling of randomly oriented crystallites.

Following initial pressurization the material was heated at 1545 ± 80 K using a CO_2 laser beam focused on the sample while monitoring the x-ray diffraction pattern [69]. After approximately 5 minutes new single-crystal spots appeared in the two-dimensional (2D) diffraction pattern that had been previously dominated by broad diffraction rings from the compressed TGCN phase and Ne PTM material [Figs. 4(a) and 4(b)]. Interestingly, the appearance of the crystalline peaks was accompanied by a pressure drop inside the DAC chamber to 44 GPa, as indicated by ruby fluorescence, as well as by an 18% lattice expansion of the solid Ne used as PTM [Fig. 4(a)]. This possibly indicates a corresponding densification within the C_3N_4 sample. Analysis of our x-ray data showed no evidence for diamond or any elemental N_2 phases formed during the experiment. There was likewise no evidence for any of the other predicted carbon nitride phases with different N/C ratios such as CN or CN_2. We conclude that the sample retained its initial composition close to C_3N_4 throughout the DAC laser heating experiment. The crystalline material produced in the experiment corresponded to only a few crystallites distributed throughout the sample. While the sample remained at high pressure in the DAC we carried out a mapping study by using a focused (∼2 micrometers) x-ray beam that revealed crystals present in only 3 out of 36 patterns obtained. A typical 2D diffraction image is shown in Fig. 4(b) showing the crystalline spots against the sharper rings from the Ne PTM and diffuse scattering from the densified disordered C_3N_4 material.

During recovery to ambient conditions the diffraction pattern emerged more clearly. Once removed from the DAC, the sample which remained mounted inside its Re gasket was examined by x-ray diffraction. Although there were more crystalline features than at high pressure, the powder averaging remained poor and it was not possible to carry out *ab initio* or Rietveld structure refinements [Fig. 4(c)]. However, we tested the range of diffraction peaks against calculated patterns for the various polymorphs produced in our AIRSS study as well as other theoretically predicted structures. Only one phase contained peaks within the range of d spacings observed experimentally. This corresponded to a new C_3N_4 polymorph with $P4_32_12$ symmetry as predicted by the AIRSS calculations. This phase is predicted by PBEsol to have a stability range between 2 and 11 GPa. At 50 GPa it is highly metastable relative to the predicted α-C_3N_4 ($P31c$) or $Pnnm$ structures, but it lies lower in energy than the metastably compressed graphitic forms (Fig. 2). We found

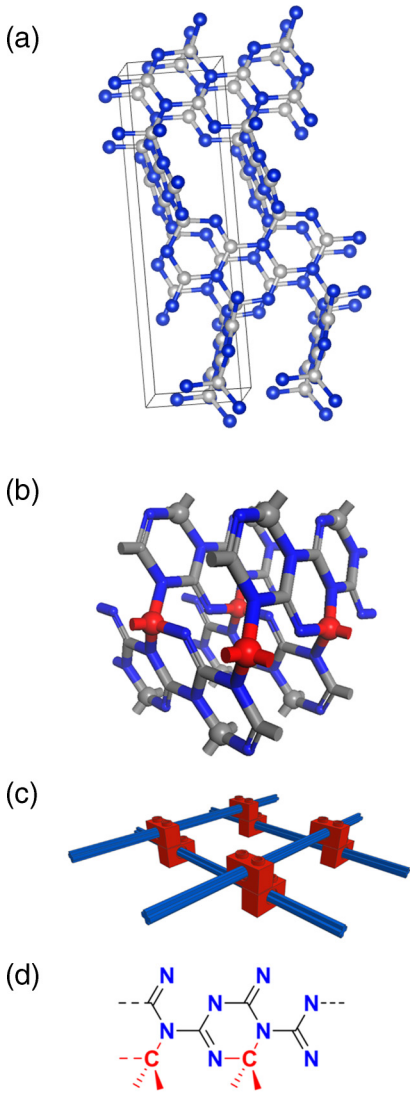

FIG. 5. Different ways of depicting the $P4_32_12$ structure. (a) Ball-and-stick model: carbon atoms (gray), nitrogen atoms (blue). (b) Structure drawing emphasizing the sp^3-bonded carbon atoms (red). (c) Abstract "Lego" representation featuring parallel, one-dimensional struts of quasi-aromatic imidamides (shown in blue) linked together by tetrahedral sp^3-bonded carbon joints (shown in red). (d) A fragment of the hybrid sp^2-sp^3-bonded carbon nitride.

an excellent match between all the observed d spacings for the new crystalline phase and predicted reflections for the $P4_32_12$ polymorph. We then used Le Bail analysis to obtain refined unit-cell parameters $a = b = 4.021$ Å, $c = 13.922$ Å, $c/a = 3.46$, and $V = 56.26$ Å^3 per f.u., with structural residual or reliability factors $R_{wp} = 6.49$ and $R_p = 4.23$ [Fig. 4(c)]. These cell parameters are in reasonable agreement with the predicted values for the new structure type at 0 GPa (Table I). The observed pattern of x-ray intensities differs substantially from those expected for a fully averaged powder diffraction pattern because only a few crystallites were present within the laser heated sample. In addition, the crystallites might exhibit preferred orientation, further complicating any more detailed analysis of the experimental data. We were able to generate patterns that approximately modelled the observed intensity distribution by constructing composites containing a few oriented crystallites with fixed atomic positions from the $P4_32_12$-theory predictions, applying a March–Dollase function to correct for preferred orientation. By using this approach, we obtained solutions to a constrained Rietveld refinement of the structure with large but not unreasonable residual values, e.g., with R_{wp} and R_p on the order of ∼20 [Fig. 4(d)].

To test the possibility that other atomic arrangements could give rise to the same unit cell we then used AIRSS to examine alternative structure solutions within the experimentally determined cell shape and volume under ambient conditions. The use of the PBEsol functional for these runs gave a very small residual pressure of about 0.4 GPa in the experimental cell while PBE indicated a pressure of 3 GPa. Our searches consistently returned $P4_32_12$ as the most stable phase, with the next possibility lying at much higher energy (0.75 eV/f.u.). We conclude from this analysis that the newly predicted $P4_32_12$ polymorph was produced in our high-pressure–high-temperature experiment. This constitutes a successful experimental synthesis of a crystalline C_3N_4 framework structure predicted by *ab initio* theory. Along with the defective-wurtzite structure C_2N_3H [31,32] and the recent report of a new CN phase [33] it constitutes a new example of a crystalline carbon-nitride-containing sp^3-bonded carbon atoms. Various schematic drawings of the new $P4_32_12$ polymorph are shown in Fig. 5 to highlight different important features of the structure. It corresponds to a new framework type containing fused triazine rings linked via sp^3-bonded C atoms. This is important because mixed sp^2/sp^3 bonding around the C atoms does not occur for pure carbon polymorphs in equilibrium at any pressure. In addition the geometrical arrangement containing sp^3-bonded carbon linked to four nitrogen atoms is highly unusual and perhaps absent in all organic chemistry except perhaps among transition states. Our experimental findings indicate that the probability of forming the new carbon nitride phase is low. This can be ascribed to high kinetic barriers as well as to the difficulty of forming the unusual C-N linked tetrahedral geometry associated with the formation reaction.

VI. STRUCTURAL COMPLEXITY AMONG CARBON NITRIDE POLYMORPHS AT LOW PRESSURE

In the low-pressure range where C_xN_y compounds are predicted to be metastable with respect to elemental carbon and nitrogen [29], it has typically been assumed by analogy with elemental carbon that layered "graphitic" motifs should constitute the ground state for carbon nitride materials at low pressures, taking into account the existence of "voids" within the layers due to the different valencies of C and N atoms [1,2,16,18–20,29,67]. One basic unit of connectivity is the planar triazine (C_3N_3) ring that may be interconnected via linking –N= bonds to form polytriazine imide (PTI) layers with C_3N_4 stoichiometry [14,16,18–20]. The polymeric TGCN material synthesized by Algara–Siller *et al.* [14] and used as the precursor for our high-pressure experiments was based on such PTI layers with either AB (space group $P\bar{6}m2$) or ABC ($P6_3cm$) stacking. The most stable TGCN polymorph found in our AIRSS study had $P6_3cm$ symmetry (Fig. 6). It

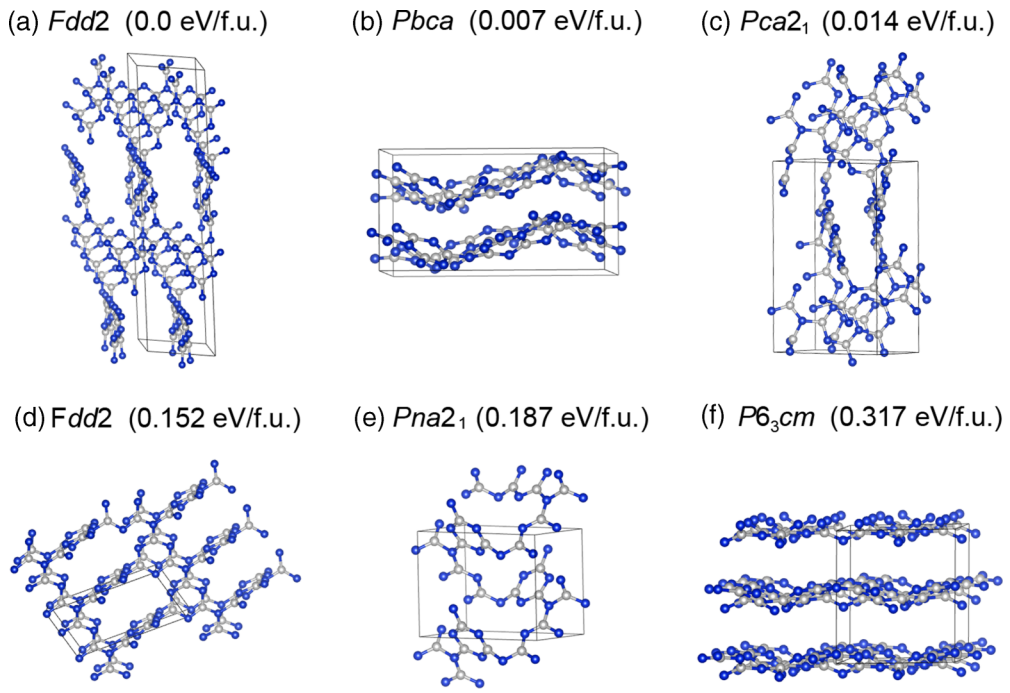

FIG. 6. Structure types observed among low-density structures ranked according to relative energy (eV/f.u.) at $P = 0$ GPa using the PBEsol functional. (a) This $ThSi_2$ heptazine-based framework with $Fdd2$ symmetry is found to be very slightly higher in energy than the ground-state PH structure of Cc symmetry at zero pressure, according to PBEsol calculations [29]. (b) Other corrugated layered PH solutions are also competitive as ambient to low-pressure ground-state structures. This $Pbca$ structure lies only 0.007 eV/f.u. above Cc. (c) Additional three-dimensional framework structures based on linked PH units containing sp^2-bonded atoms are also present at low energy. Here we show an example of a $Pca2_1$ symmetry polymorph occurring at 0.014 eV/f.u. above the ground state. (d) Beginning at 0.152 eV/f.u. above the ground-state framework structures based on polytriazine imide-linked (PTI) units begin to appear. (e) The $Pna2_1$ structure found by AIRSS represents a new example of this PTI structure type. (f) At approximately 0.317 eV/f.u. above the ground state, PTI corrugated layered structures make their appearance. Here we show the $P6_3cm$ version of the TGCN structure used as a starting compound in our laser heated DAC experiments.

is predicted to lie at 0.329 eV/f.u. above the ground state at ambient pressure (see supplemental Table I). It has been shown that layers based on linked tri-*s*-triazine (polyheptazine: PH) units are more stable than the PTI motifs [1,67]. Various levels of complexity can appear among both PTI and PH connectivity patterns within a single layer, and the layers are predicted to be far from planar. Substantial buckling around the bridging –N= units that act as mechanical hinges lead to structural models with "corrugated" layers [67].

Dong *et al.* [29] found a Cc structure to be the ground state at 0 GPa, and we have found a very similar structure of $Fdd2$ symmetry that is only a fraction of an meV per f.u. higher in energy than Cc (see Fig. 6 and supplemental material [62]). We have also found a new corrugated PH structure of $Pbca$ symmetry that is predicted to be about 7 meV per f.u. higher in energy than Cc and on analysis is the same as a structure found by Gracia and Kroll but in a larger unit cell with $P1$ symmetry. We predict that $Pbca$ is the most stable phase in the range 0.05–2 GPa. The Cc, $Fdd2$, and $Pbca$ structures are based on the $ThSi_2$ motif [67]. The $Pbca$ phase, which has a starting volume near 73 Å^3/f.u. is expected to cross the $P6_3cm$ enthalpy-pressure curve at approximately 25 GPa and so would not be accessible to the experimental synthesis procedure (Fig. 2). Gracia and Kroll [67] noted tubular PH structures that could lead to macroscopic forms analogous to carbon nanotubes.

Many of these structure types have very large unit-cell volumes (>100 Å^3/f.u.) that are rapidly destabilized at high pressure; see Fig. 2. Others with energies up to 1 eV/f.u. above the ground state have volumes in the 65–90 Å^3/f.u. range and they appear as metastable structure solutions in Fig. 3. One structure stands out: This is the new $P4_32_12$ phase described above that we have synthesized experimentally (Fig. 5). The experimental volume of $P4_32_12$ of 56.26 Å^3/f.u. is a little smaller than the PBEsol volume of 59.97 Å^3/f.u.

A further new phase of $Fdd2$ symmetry consisting of triazine rings linked into a three-dimensional framework via sp^2-bonded atoms is found to occur at 0.152 eV/f.u. above the ground state at ambient pressure (Fig. 6). The identification of such a new family of framework structures built from thermally stable C–N bonds opens up new directions for carbon nitride research. The challenge for carbon nitride synthesis is now to produce some of these predicted phases and their unusual bonded architectures in a controlled way, and verify their structures and determine their properties experimentally.

Of particular interest is the behavior of the $P6_3cm$ phase that forms the main constituent of TGCN used as a starting material for our laser heated diamond anvil cell experiments. At ambient pressure it lies at 0.317 eV/f.u. above the ground state and at approximately 0.2 eV/f.u. above $P4_32_12$; see Fig. 2. During initial compression the TGCN phase loses its initial crystallinity but it can be expected to continue along a similar

enthalpy-pressure path to reach approximately 0.5 eV/f.u. above the $P4_32_12$ energy by 50 GPa. By this pressure $P4_32_12$ has become substantially metastable (by ∼3 eV/f.u.) relative to α-C_3N_4 and other dense phases but it is the next lowest in enthalpy that we have found following destabilization of the disordered and metastably compressed $P6_3cm$ material.

These predicted results can allow us to better understand the nucleation of only a few crystals of the $P4_32_12$ phase following laser heating within the metastably compressed $P6_3cm$ TGCN compound. Interestingly, several other C_3N_4 polymorphs are also predicted to occur within the 20–80 GPa pressure range, with enthalpies extending to ∼0.5 eV/f.u. above the ground state. We might expect that further high-P, -T experiments carried out on metastably compressed starting materials could lead to identification of these new C_3N_4 polymorphs.

VII. CONCLUSIONS

Extended sp^2-bonded framework and layered carbon nitride structures are found to be thermodynamically stable at pressures below about 2 GPa. The lowest-energy structures are built from linked polyheptazine (PH) units: at higher energies layered and three-dimensional (3D) microporous frameworks based on triazine rings linked by imide groups (PTI structures) appear. The enthalpies and volumes per f.u. are reported in the supplemental material [62].

We find that the microporous PH Cc structure is the most stable at zero pressure, although the similar $Fdd2$ structure is only a fraction of an meV per f.u. higher in energy. A layered $Pbca$ PH structure is predicted to be stable in the range 0.05–2 GPa.

The $P4_32_12$ structure is a new structure prototype not found in databases that we have discovered using AIRSS. It has mixed sp^2 and sp^3 bonding and is predicted to be stable in the range 2–11 GPa. C_3N_4 therefore differs from pure carbon in that there is a thermodynamically stable phase between the sp^2- and sp^3-bonded forms. This structure could be accessible through suitable precursors and synthetic routes at low pressure.

All of the predicted thermodynamically stable phases at pressures above 11 GPa consist entirely of four-fold-coordinated C atoms and three-fold-coordinated N atoms.

The relative stabilities of the most favorable C_3N_4 have uncertainties due to the use of approximate density functionals which amount to a few GPa at low pressures. We have, however, sought to assess the sizes of these errors by comparing with results for the related carbon graphite-diamond transition.

AIRSS has predicted new $Pbca$, $P4_32_12$, $Pnnm$, $Pmc2_1$, and $Pnma$ C_3N_4 structures to have regions of thermodynamic stability and, in addition, the new $Fdd2$ structure is almost stable. Our calculations predict decomposition of C_3N_4 at pressures above 650 GPa into diamond and pyrite-structured CN_2.

Our experimental study has provided strong evidence for the synthesis in laser-heated diamond anvil cell experiments of the newly predicted $P4_32_12$ structure. The identification of a new family of structures with mixed sp^2 and sp^3 bonding opens up a new area of exploration for these important photo- and catalytically active solid materials.

ACKNOWLEDGMENTS

R.J.N. acknowledges financial support from the Engineering and Physical Sciences Research Council (EPSRC) of the U.K. [EP/J017639/1]. C.J.P. acknowledges financial support from EPSRC [EP/G007489/2] and [EP/K013688/1], and a Royal Society Wolfson Research Merit Award. R.J.N. and C.J.P. acknowledge use of the Archer facilities of the U.K.'s national high-performance computing service (for which access was obtained via the UKCP consortium [EP/K013688/1] and [EP/K014560/1]). P.F.M. was supported by EPSRC Grant [EP/L01709/1]. M.J.B. thanks the Czech Science Foundation (GA ČR) for junior grant funding (CAMs – 16-21151Y) and the European Research Council (ERC) for funding under the Starting Grant scheme (BEGMAT – 678462).

[1] E. Kroke and M. Schwarz, Novel group 14 nitrides, Coord. Chem. Rev. **248**, 493 (2004).

[2] A. Schwarzer, T. Saplinova, and E. Kroke, Tri-*s*-triazines (*s*-heptazines)–from a "mystery molecule" to industrially relevant carbon nitride materials, Coord. Chem. Rev. **257**, 2032 (2013).

[3] A. Thomas, A. Fischer, F. Goettmann, M. Antonietti, J.-O. Müller, R. Schlögle, and J. M. Carlsson, Graphitic carbon nitride materials: Variation of structure and morphology and their use as metal-free catalysts, J. Mater. Chem. **18**, 4893 (2008).

[4] G. Goglio, D. Foy, and G. Demazeau, State of art and recent trends in bulk carbon nitrides synthesis, Mater. Sci. Eng., R **58**, 195 (2008).

[5] T. Malkow, Critical observations in the research of carbon nitride, Mater. Sci. Eng., A **292**, 112 (2000).

[6] X. Wang, K. Maeda, A. Thomas, K. Takanabe, G. Xin, J. M. Carlsson, K. Domen, and M. Antonietti, A metal-free polymeric photocatalyst for hydrogen production from water under visible light, Nat. Mater. **8**, 76 (2009).

[7] B. V. Lotsch, M. Döblinger, J. Sehnert, L. Seyfarth, J. Senker, O. Oeckler, and W. Schnick, Unmasking melon by a complementary approach employing electron diffraction, solid-state NMR spectroscopy, and theoretical calculations–structural characterization of a carbon nitride polymer, Chem. - Eur. J. **13**, 4969 (2007).

[8] B. Jurgens, E. Irran, J. Senker, P. Kroll, H. Muller, and W. Schnick, Melem (2, 5, 8-triamino-tri-*s*-triazine), an important intermediate during condensation of melamine rings to graphitic carbon nitride: Synthesis, structure determination by x-ray powder diffractometry, solid-state NMR, and theoretical studies, J. Am. Chem. Soc. **125**, 10288 (2003).

[9] B. V. Lotsch and W. Schnick, New light on an old story: Formation of melam during thermal condensation of melamine, Chem. - Eur. J. **13**, 4956 (2007).

[10] M. J. Bojdys, J.-O. Mueller, M. Antonietti, and A. Thomas, Ionothermal synthesis of crystalline, condensed, graphitic carbon nitride, Chem. - Eur. J. **14**, 8177 (2008).

[11] E. Wirnhier, M. Döblinger, D. Gunzelmann, J. Senker, B. V. Lotsch, and W. Schnick, Poly(triazine imide) with intercalation of lithium and chloride ions $[(C_3N_3)_2(NH_xLi_{1-x})_3 \cdot LiCl]$: A crystalline 2D carbon nitride network, Chem. - Eur. J. **17**, 3213 (2011).

[12] S. Y. Chong, J. T. A. Jones, Y. Z. Khimyak, A. I. Cooper, A. Thomas, M. Antonietti, and M. J. Bojdys, Tuning of gallery heights in a crystalline 2D carbon nitride network, J. Mater. Chem. A **1**, 1102 (2013).

[13] Z. Zhang, K. Leinenweber, Matt Bauer, Laurence A. J. Garvie, P. F. McMillan, and G. H. Wolf, High-pressure bulk synthesis of crystalline $C_6N_9H_3 \cdot HCl$: a novel C_3N_4 graphitic derivative, J. Am. Chem. Soc. **123**, 7788 (2001).

[14] G. Algara-Siller, N. Severin, S. Y. Chong, T. Björkman, R. G. Palgrave, A. Laybourn, M. Antonietti, Y. Z. Khimyak, A. V. Krasheninnikov, J. P. Rabe, U. Kaiser, A. I. Cooper, A. Thomas, and M. J. Bojdys, Triazine-based graphitic carbon nitride: A two-dimensional semiconductor, Angew. Chem., Int. Ed. **53**, 7450 (2014).

[15] A. Y. Liu and R. M. Wentzcovitch, Stability of carbon nitride solids, Phys. Rev. B **50**, 10362 (1994).

[16] D. M. Teter and R. J. Hemley, Low-compressibility carbon nitrides, Science **271**, 53 (1996).

[17] M. Todd, J. Kouvetakis, T. L. Groy, D. Chandrasekhar, D. J. Smith, and P. W. Deal, Novel synthetic routes to carbon nitride, Chem. Mater. **7**, 1422 (1995).

[18] J. Kouvetakis, M. Todd, B. Wilkens, A. Bandari, and N. Cave, Novel synthetic routes to carbon-nitrogen thin films, Chem. Mater. **6**, 811 (1994).

[19] J. Ortega and O. F. Sankey, Relative stability of hexagonal and planar structures of hypothetical C_3N_4 solids, Phys. Rev. B **51**, 2624 (1995).

[20] J. E. Lowther, Relative stability of some possible phases of graphitic carbon nitride, Phys. Rev. B **59**, 11683 (1999).

[21] M. J. Bojdys, N. Severin, J. P. Rabe, A. I. Cooper, A. Thomas, and M. Antonietti, Exfoliation of crystalline 2D carbon nitride: thin sheets, scrolls and bundles via mechanical and chemical routes, Macromol. Rapid Commun. **34**, 850 (2013).

[22] T. Y. Ma, Y. Tang, S. Dai, and S. Z. Qiao, Proton-functionalized two-dimensional graphitic carbon nitride nanosheet: An excellent metal-/label-free biosensing platform, Small **10**, 2382 (2014).

[23] M. Deifallah, P. F. McMillan, and F. Cora, Electronic and structural properties of two-dimensional carbon nitride graphenes, J. Phys. Chem. C **112**, 5447 (2008).

[24] S. Zuluaga, L. H. Liu, N. Shafiq, S. M. Rupich, J.-F. Veyan, Y. J. Chabal, and T. Thonhauser, Structural band-gap tuning in g-C_3N_4, Phys. Chem. Chem. Phys. **17**, 957 (2015).

[25] M. L. Cohen, Calculation of bulk moduli of diamond and zinc-blende solids, Phys. Rev. B **32**, 7988 (1985).

[26] A. Y. Liu and M. L. Cohen, Prediction of new low compressibility solids, Science **245**, 841 (1989).

[27] A. Y. Liu and M. L. Cohen, Structural properties and electronic structure of low-compressibility materials: β-Si_3N_4 and hypothetical β-C_3N_4, Phys. Rev. B **41**, 10727 (1990).

[28] C.-M. Sung and M. Sung, Carbon nitride and other speculative superhard materials, Mater. Chem. Phys. **43**, 1 (1996).

[29] H. Dong, A. R. Oganov, Q. Zhu, and G.-R. Qian, The phase diagram and hardness of carbon nitrides, Sci. Rep. **5**, 9870 (2015).

[30] E. Kroke, gt-C_3N_4–the first stable binary carbon(IV) nitride, Angew. Chem., Int. Ed. **53**, 11134 (2014).

[31] E. Horvath-Bordon, R. Riedel, P. F. McMillan, P. Kroll, G. Miehe, P. A. van Aken, A. Zerr, P. Hoppe, O. Shebanova, I. McLaren, S. Lauterbach, E. Kroke, and R. Boehler, High-pressure synthesis of crystalline carbon nitride imide, $C_2N_2(NH)$, Angew. Chem., Int. Ed. **46**, 1476 (2007).

[32] A. Salamat, K. Woodhead, P. F. McMillan, R. Q. Cabrera, A. Rahman, D. Adriaens, F. Cora, and J.-P. Perrillat, Tetrahedrally bonded dense C_2N_3H with a defective wurtzite structure: X-ray diffraction and Raman scattering results at high pressure and ambient conditions, Phys. Rev. B **80**, 104106 (2009).

[33] E. Stavrou, S. Lobanov, H. Dong, A. R. Oganov, V. B. Prakapenka, Z. Konopkova, and A. F. Goncharov, Synthesis of Ultra-Incompressible sp^3-Hybridized Carbon Nitride, arXiv:1412.3755.

[34] A. Salamat, M. Deifallah, R. Q. Cabrera, F. Cora, and P. F. McMillan, Identification of new pillared-layered carbon nitride materials at high pressure, Sci. Rep. **3**, 2122 (2013).

[35] D. T. Vodak, K. Kim, L. Iordanidis, P. G. Rasmussen, A. J. Matzger, and O. M. Yaghi, Computation of aromatic C_3N_4 networks and synthesis of the molecular precursor $N(C_3N_3)_3Cl_6$, Chem. - Eur. J. **9**, 4197 (2003).

[36] S. Ren, M. J. Bojdys, R. Dawson, A. Laybourn, Y. Z. Khimyak, D. J. Adams, and A. I. Cooper, Porous, fluorescent, covalent triazine-based frameworks via room-temperature and microwave-assisted synthesis, Adv. Mater. **24**, 2357 (2012).

[37] M. J. Bojdys, J. Jeromenok, A. Thomas, and M. Antonietti, Rational extension of the family of layered, covalent, triazine-based frameworks with regular porosity, Adv. Mater. **22**, 2202 (2010).

[38] H.-J. Li, B.-W. Sun, L. Sui, D.-J. Qian, and M. Chen, Preparation of water-dispersible porous g-C_3N_4 with improved photocatalytic activity by chemical oxidation, Phys. Chem. Chem. Phys. **17**, 3309 (2015).

[39] C. Reece, D. J. Willock, and A. Trewin, Modelling analysis of the structure and porosity of covalent triazine-based frameworks, Phys. Chem. Chem. Phys. **17**, 817 (2015).

[40] A. R. Oganov, R. J. Hemley, R. M. Hazen, and A. P. Jones, Structure, bonding, and mineralogy of carbon at extreme conditions, Rev. Mineral. Geochem. **75**, 47 (2013).

[41] Y. Gong, Z. Wei, J. Wang, P. Zhang, H. Li, and Y. Wang, Design and fabrication of hierarchically porous carbon with a template-free method, Sci. Rep. **4**, 6349 (2014).

[42] M. Lazzeri and A. Barreiro, Carbon-based nanoscience, Elements (Chantilly, VA, U. S.) **10**, 447 (2014).

[43] I. A. Baburin, D. M. Proserpio, V. A. Saleev, and A. V. Shipilova, From zeolite nets to sp^3 carbon allotropes: A topology-based multiscale theoretical study, Phys. Chem. Chem. Phys. **17**, 1332 (2015).

[44] F. P. Bundy, H. P. Bovenkerk, H. M. Strong, and R. H. Wentorf Jr., Diamond-graphite equilibrium line from growth and graphitization of diamond, J. Chem. Phys. **35**, 383 (1961).

[45] R. Z. Khaliullin, H. Eshet, T. D. Kühne, J. Behler, and M. Parrinello, Nucleation mechanism for the direct graphite-to-diamond phase transition, Nat. Mater. **10**, 693 (2011).

[46] M. Martinez-Canales, C. J. Pickard, and R. J. Needs, Thermodynamically Stable Phases of Carbon at Multiterapascal Pressures, Phys. Rev. Lett. **108**, 045704 (2012).

[47] R. F. Smith, J. H. Eggert, R. Jeanloz, T. S. Duffy, D. G. Braun, J. R. Patterson, R. E. Rudd, J. Biener, A. E. Lazicki, A. V. Hamza, J. Wang, T. Braun, L. X. Benedict, P. M. Celliers, and G. W. Collins, Ramp compression of diamond to five terapascals, Nature (London) **511**, 330 (2014).

[48] C. J. Pickard and R. J. Needs, Piling up the pressure, Nature (London) **511**, 294 (2014).

[49] C. J. Pickard and R. J. Needs, High-Pressure Phases of Silane, Phys. Rev. Lett. **97**, 045504 (2006).

[50] C. J. Pickard and R. J. Needs, *Ab initio* random structure searching, J. Phys.: Condens. Matter **23**, 053201 (2011).

[51] C. J. Pickard and R. J. Needs, Structure of phase III of solid hydrogen, Nat. Phys. **3**, 473 (2007).

[52] C. J. Pickard, M. Martinez-Canales, and R. J. Needs, Density functional theory study of phase IV of solid hydrogen, Phys. Rev. B **85**, 214114 (2012); **86**, 059902(E) (2012).

[53] S. Ninet, F. Datchi, P. Dumas, M. Mezouar, G. Garbarino, A. Mafety, C. J. Pickard, R. J. Needs, and A. M. Saitta, Experimental and theoretical evidence for an ionic crystal of ammonia at high pressure, Phys. Rev. B **89**, 174103 (2014).

[54] A. D. Fortes, E. Suard, M.-H. Lemee-Cailleau, C. J. Pickard, and R. J. Needs, Crystal structure of ammonia monohydrate II, J. Am. Chem. Soc. **131**, 13508 (2009).

[55] G. I. G. Griffiths, A. D. Fortes, C. J. Pickard, and R. J. Needs, Crystal structure of ammonia dihydrate II, J. Chem. Phys. **136**, 174512 (2012).

[56] C. J. Pickard and R. J. Needs, Metallization of aluminum hydride at high pressures: A first-principles study, Phys. Rev. B **76**, 144114 (2007).

[57] A. Dewaele, N. G. Worth, C. J. Pickard, R. J. Needs, S. Pascarelli, O. Mathon, M. Mezouar, and T. Irifune, Synthesis and stability of xenon oxides Xe_2O_5 and Xe_3O_2 under pressure, Nat. Chem. **8**, 784 (2016).

[58] L. Pauling, The principles determining the structure of complex ionic crystals, J. Am. Chem. Soc. **51**, 1010 (1929).

[59] S. J. Clark, M. D. Segall, C. J. Pickard, P. J. Hasnip, M. I. J. Probert, K. Refson, and M. C. Payne, First principles methods using CASTEP, Z. Kristallogr. **220**, 567 (2005).

[60] D. Vanderbilt, Soft self-consistent pseudopotentials in a generalized eigenvalue formalism, Phys. Rev. B **41**, 7892 (1990).

[61] J. P. Perdew, K. Burke, and M. Ernzerhof, Generalized Gradient Approximation Made Simple, Phys. Rev. Lett. **77**, 3865 (1996); **78**, 1396(E) (1997).

[62] See Supplemental Material at http://link.aps.org/supplemental/10.1103/PhysRevB.94.094104 for additional information about the C_3N_4 structures.

[63] W. Kohn and L. J. Sham, Self-consistent equations including exchange and correlation effects, Phys. Rev. **140**, A1133 (1965).

[64] Z. Wu and R. E. Cohen, More accurate generalized gradient approximation for solids, Phys. Rev. B **73**, 235116 (2006).

[65] J. P. Perdew, A. Ruzsinszky, G. I. Csonka, O. A. Vydrov, G. E. Scuseria, L. A. Constantin, X. Zhou, and K. Burke, Restoring the Density-Gradient Expansion for Exchange in Solids and Surfaces, Phys. Rev. Lett. **100**, 136406 (2008); **102**, 039902(E) (2009).

[66] S. Grimme, Semiempirical GGA-type density functional constructed with a long-range dispersion correction, J. Comput. Chem. **27**, 1787 (2006).

[67] J. Gracia and P. Kroll, Corrugated layered heptazine-based carbon nitride: the lowest energy modifications of C_3N_4 ground state, J. Mater. Chem. **19**, 3013 (2009).

[68] Y. Guo and W. A. Goddard III, Is carbon nitride harder than diamond? No, but its girth increases when stretched (negative Poisson ratio), Chem. Phys. Lett. **237**, 72 (1995).

[69] S. Petitgirard, A. Salamat, P. Beck, G. Weck, and P. Bouvier, Strategies for *in situ* laser heating in the diamond anvil cell at an x-ray diffraction beamline, J. Synchrotron Radiat. **21**, 89 (2014).